Supporting Information: In Situ Nanoparticle Sizing with Zeptomole Sensitivity

Christopher Batchelor-McAuley[a], Joanna Ellison[a], Kristina Tschulik[a], Philip L. Hurst[a], Regine Boldt[b], Richard G. Compton[a]*

[a] Department of Chemistry, Physical and Theoretical Chemistry Laboratory, University of Oxford, South Parks Road, Oxford OX1 3QZ, United Kingdom

[b]Leibniz-Institut für Polymerforschung Dresden e.V. Hohe Str. 6, 01069 Dresden, Germany

[*]Corresponding author. Fax: +44(0) 1865 275957
Email address: richard.compton@chem.ox.ac.uk

Section 1: Potentiostat results

The following section presents the power spectra density noise data, quantifying the performance of the device.

Figure 1 compares the input referred current noise for the low-noise amplifier and potentiostat used within this text and two commercial potentiostat systems. The low-noise potentiostat (black line figure 1) in the absence of filtering has a bandwidth of 4kHz and the amplifier output was digitised at 30kHz. As can be seen the noise profile is flat up to 1kHz with a value of ~4 A^2/Hz. Conversely, the two commercial systems have a fixed upper bandwidth (in the 10nA current range) of only 100 Hz (the presented data has been sampled at 2 kHz). At lower frequencies, it can be seen that the noise density associated with both commercial systems is over an order of magnitude larger than that of the low-noise potentiostat used within this work. Moreover, no significant roll-off in the noise is seen at 100 Hz, implying that the noise floor for these commercial systems is not determined by the current-amplifier but is more likely related to the analog-to-digital converter.
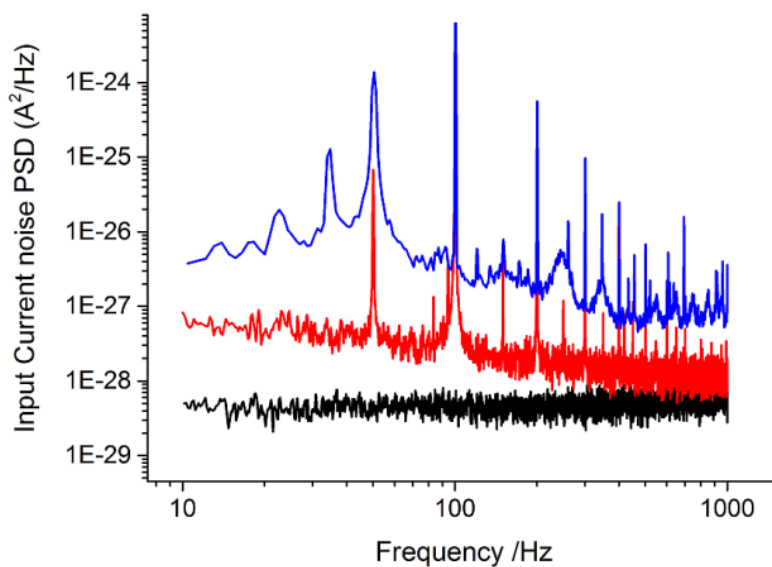
Figure 1: Current power spectral density of different potentiostats: Black, in house built low noise potentiostat; Red, autolab type II; Blue, autolab type III

Figure 2, depicts the response of the low noise potentiostat measuring the current noise response across a 100 Mohm resistor in the presence and absence of the 250 Hz low-pass 4-pole Bessel filter used within the impact experiments. From equation 1 in the main text the thermal current noise PSD across a 100 Mohm resistor is predicted to be 1.6×10^{-28} A^2/Hz (plotted as the solid line in figure 2). The measured noise current (dashed line,

~2x10^{-28} A^2/Hz) is marginally above this theoretically predicted value. The difference originates from the addition of the current-amplifier noise (4x10^{-29} A^2/Hz) to the thermal noise across the resistor. Where,

$$Var(i_{noise,total}) = Var(i_{noise,amplifier}) + Var(i_{noise,resistor})$$

The red trace in Figure 2 depicts the input current noise for the system with additional 250 Hz (4-pole Bessel) filtering, as can be seen significant roll-off of the noise power is recorded at higher frequencies.
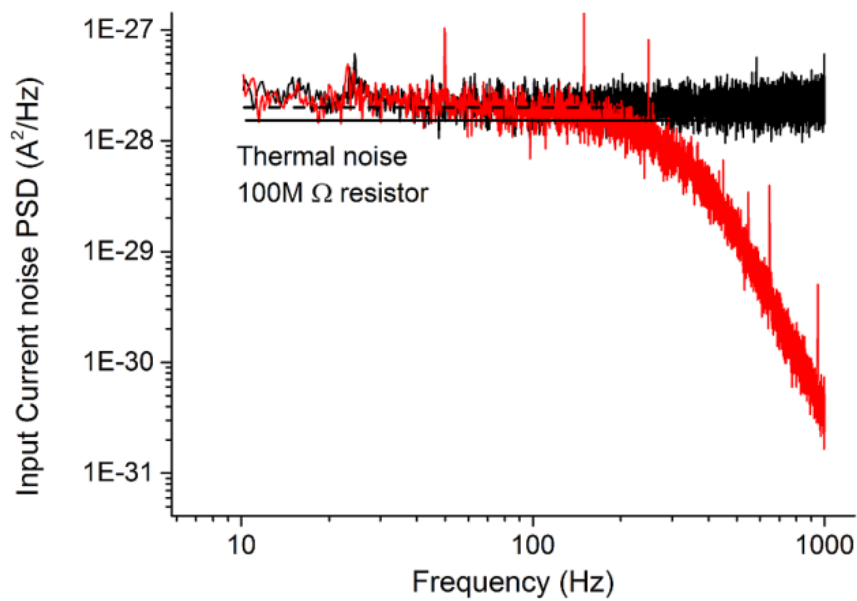
Figure 2: Power spectral density of the system with no filter (black) and a 250 Hz 4-pole Bessel filter (red)

Section 2: Nanoparticle Impact results

Nanoparticle impact results
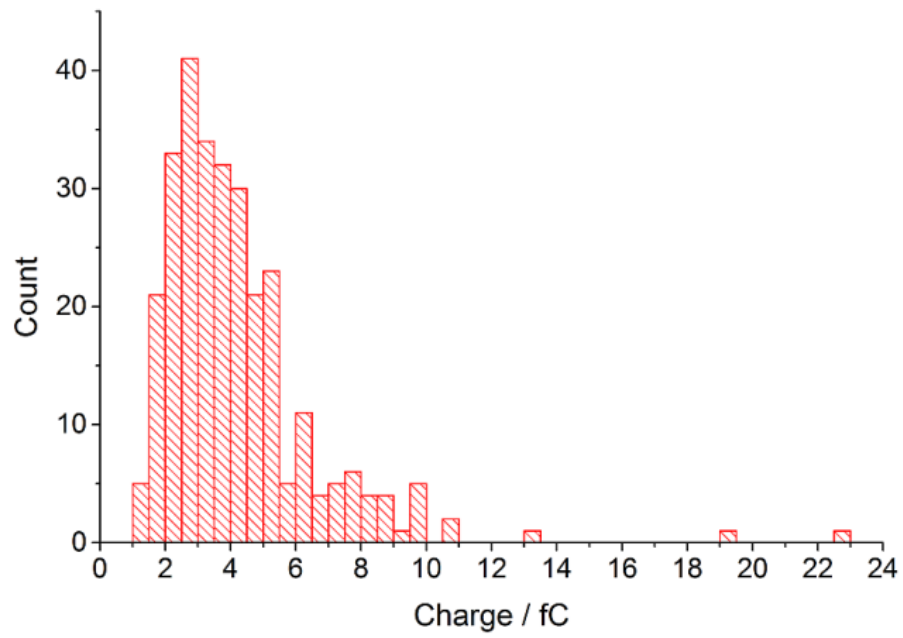
Figure 3: A histogram showing the charge distribution for the oxidation of AgNPs impacting the electrode

Section 3: Electrode Characterisation

Electrochemical results:
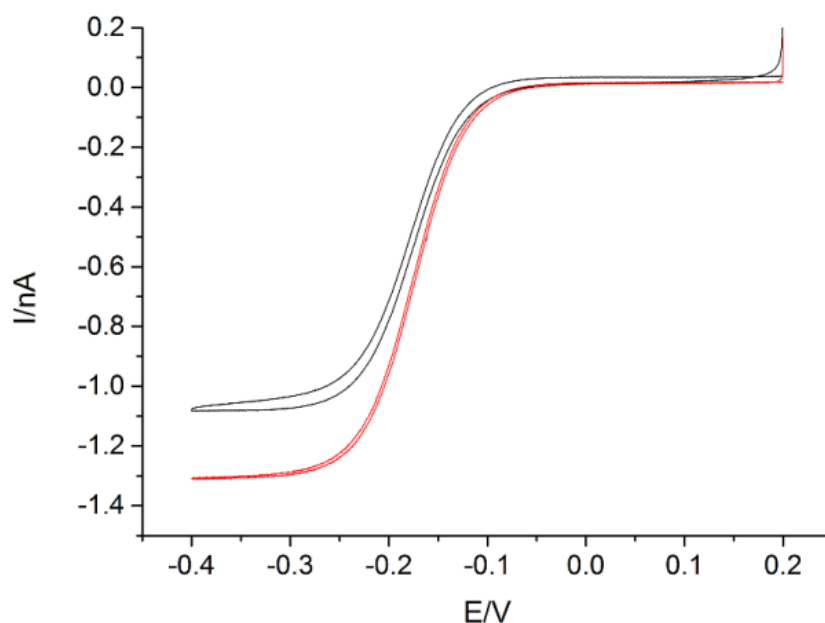
Figure 4: Cyclic voltammograms in 1.0 mM hexamine ruthenium chloride with 0.1 M KCl supporting electrolyte at 25 mVs^{-1}. Black line shows a commercial, glass insulated electrode and the red line shows the fabricated polymer coated electrode.

Characterisation of the electrodes was performed in 1 mM hexamine ruthenium chloride with 0.1 M KCl as supporting electrolyte. The solution was thoroughly degassed by purging with nitrogen and thermostated to 25 ± 0.5 °C. A three electrode system was used consisting of either the fabricated micro-disc electrode or a commercial 7 μm diameter carbon micro electrode (BASi Inc), a platinum mesh counter electrode and a saturated calomel reference electrode (SCE, potential E = 0.244 V versus standard hydrogen electrode). The commercial carbon fibre was polished on decreasing grade (1, 0.3, 0.05 μm diameter) of alumina powder before experiments. Cyclic voltammograms were run using a μAutolab II potentiostat (Metrohm-Autolab BV, Utrecht, Netherlands) from a potential of 0.2 V to -0.4 V vs SCE at 25 mVs^{-1}. Scans were run on both a glass coated commercial micro-electrode and the fabricated electrode, in order to determine the difference in capacitance of the two systems.

Cyclic voltammograms of both the commercial and the fabricated carbon fibre microelectrodes demonstrate steady state voltammograms corresponding to the reduction of the $[Ru(NH_3)_6]^{3+}$. The commercial carbon microelectrode gives a steady state current value of 1.08 nA, corresponding to an electrode radius of 3.32 μm. The increased current for the polymer coated electrode represents the enhanced mass transport at the disc edges for an electrode with a thin sheath. The voltammograms also demonstrate the enhanced capacitance of the commercial microelectrode due to its increased surface roughness.

SEM results:
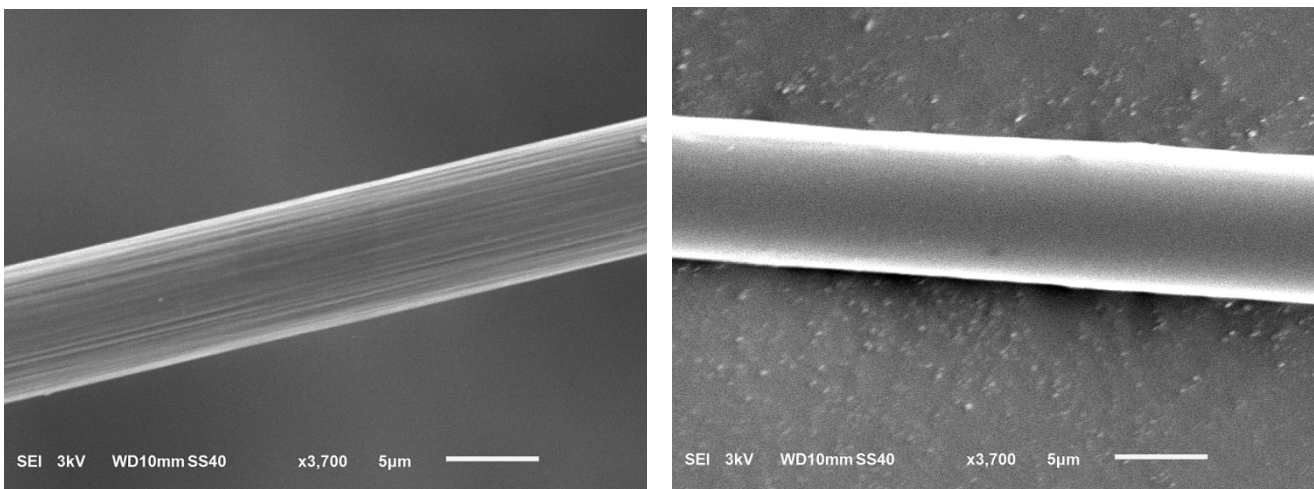
Figure 5: SEM image of a) an uncoated carbon fibre and b) a polymer coated carbon fibre

SEM images show that the carbon fibre initially has a rough surface. This is then fully covered by the polymer coating during the insulation stage of the fabrication. The coating covers the whole carbon fibre and was found to be relatively uniform across the whole carbon fibre surface and was found to be of the order of 200-2000 nm in thickness.

Section 4: Nanoparticle Characterisation

UV-Vis spectroscopy:
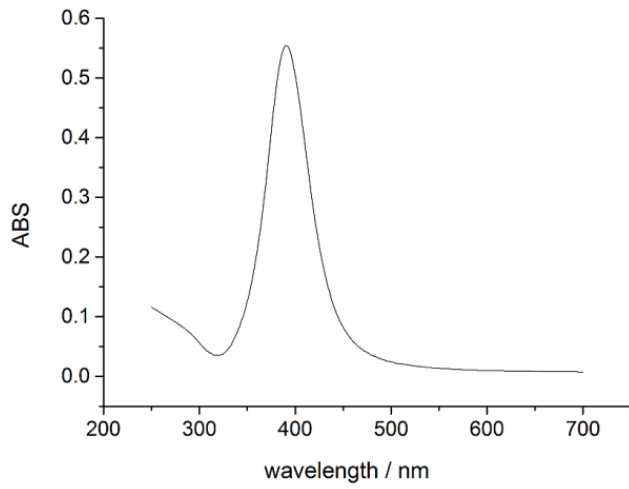
Figure 6: UV-Vis spectrum of the synthesised nanoparticles, demonstrating a maximum absorbance at 390 nm.

TEM Images
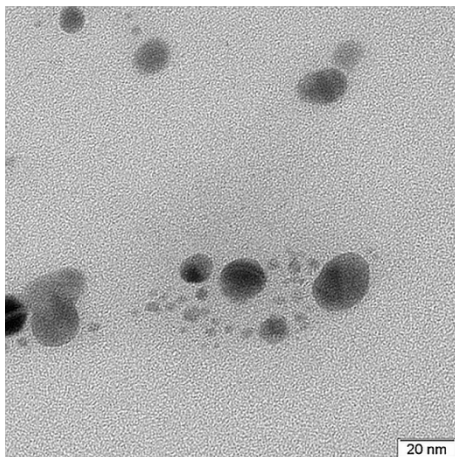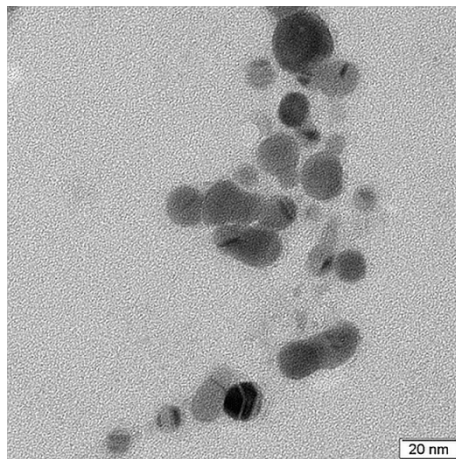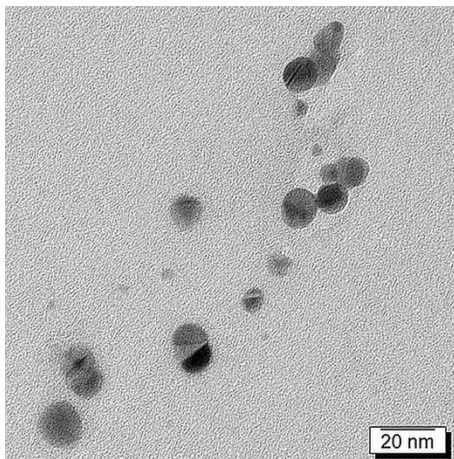
DLS:

Figure 7: TEM images of the synthesised silver nanoparticles
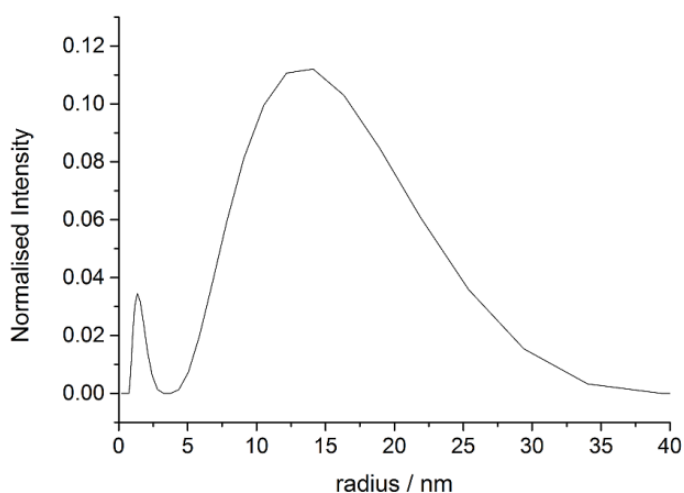
Figure 8: Normalised intensity plot of DLS data of the silver nanoparticles

The DLS data of the synthesised silver nanoparticles shows a bimodal distribution, indicating the presence of small and large populations of silver nanoparticles. It should be noted that the intensity readings obtained via DLS are heavily weighted towards the detection of larger nanoparticles, with Rayleigh scattering having an inverse of r^6 dependency. Therefore the true size distribution of the sample will show increased numbers of the small nanoparticles and a reduction in the number of larger nanoparticles.